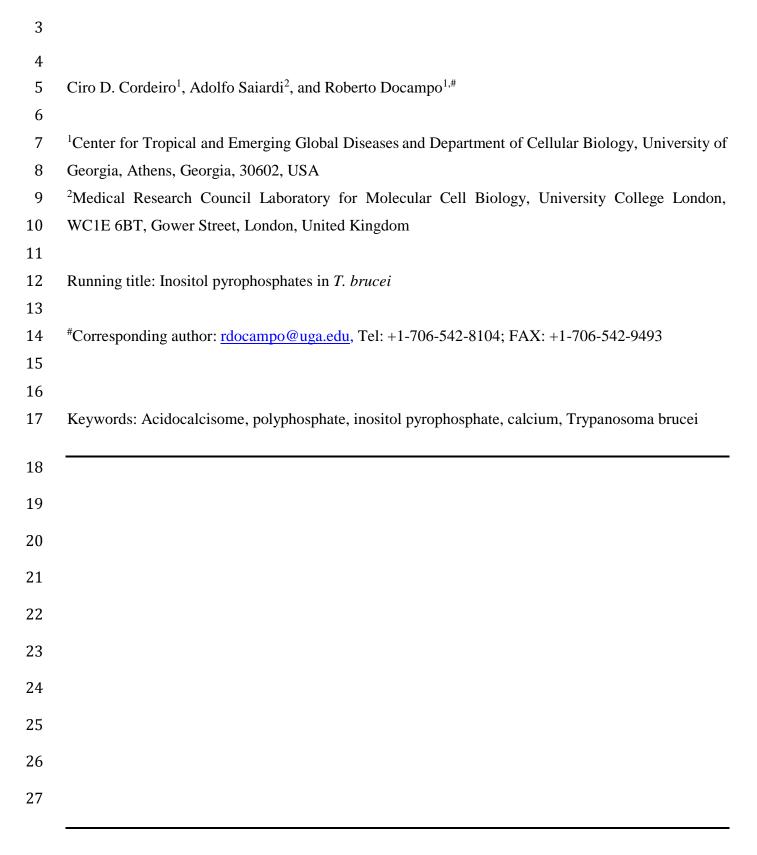
- 1 The inositol pyrophosphate synthesis pathway in *Trypanosoma*
- 2 brucei is linked to polyphosphate synthesis in acidocalcisomes



Summary

28

29

30

31

32

33

34

35

36

37

38

39

40

41

42

Inositol pyrophosphates are novel signaling molecules possessing high-energy pyrophosphate bonds and involved in a number of biological functions. Here, we report the correct identification and characterization of the kinases involved in the inositol pyrophosphate biosynthetic pathway in Trypanosoma brucei: inositol polyphosphate multikinase (TbIPMK), inositol pentakisphosphate 2kinase (TbIP5K) and inositol hexakisphosphate kinase (TbIP6K). TbIP5K and TbIP6K were not identifiable by sequence alone and their activities were validated by enzymatic assays with the recombinant proteins or by their complementation of yeast mutants. We also analyzed T. brucei extracts for the presence of inositol phosphates using polyacrylamide gel electrophoresis and high performance liquid chromatography. Interestingly, we could detect inositol phosphate (IP), inositol 4,5-bisphosphate (IP₂), inositol 1,4,5-trisphosphate (IP₃) and inositol hexakisphosphate (IP₆) in T. brucei different stages. Bloodstream forms unable to produce inositol pyrophosphates, due to downregulation of TbIPMK expression by conditional knockout, have reduced levels of polyphosphate and altered acidocalcisomes. Our study links the inositol pyrophosphate pathway to the synthesis of polyphosphate in acidocalcisomes, and may lead to better understanding of these organisms and provide new targets for drug discovery.

44

45

46

47

48

49

50

51

52

43

Introduction

Myo-inositol is an essential precursor for the synthesis of soluble inositol phosphates (IPs) and lipid-bound inositols called phosphoinositides (PIPs) (Irvine *et al.*, 2001). After inositol incorporation into the lipid phosphatidylinositol (PI), the inositol ring is phosphorylated to PIPs such as phosphatidylinositol 4,5-bisphosphate (PIP₂) through the action of a phosphatidylinositol phosphate (PIP) kinase. PIP₂ is cleaved by a phosphoinositide phospholipase C (PI-PLC) (Cocco *et al.*, 2015) to inositol 1,4,5-trisphosphate (IP₃) (Fig. 1) and 1,2-diacylglycerol (DAG), which are important second messengers. While DAG stimulates a protein kinase C (Nishizuka, 1986), IP₃ stimulates an IP₃

receptor to release Ca²⁺ from intracellular stores (Berridge, 2009) and can be further metabolized to other soluble IPs by several kinases and phosphatases.

53

54

55

56

57

58

59

60

61

62

63

64

65

66

67

68

69

70

71

72

73

74

75

76

77

The inositol phosphate multikinase (IPMK) has dual 3-kinase/6-kinase activity and catalyzes the conversion of IP₃ into inositol tetrakisphosphate (IP₄) and inositol pentakisphosphate (IP₅). IP₅ is converted into inositol hexakisphosphate (IP₆), the fully phosphorylated myo-inositol also known as phytic acid, by the 2-kinase activity of inositol pentakisphosphate kinase (IP5K, or IPPK). Further phosphorylation of IP₆ by the inositol hexakisphosphate kinase (IP₆ kinase or IP₆K) results in the production of diphosphoinositol polyphosphates (PP-IPs), also known as inositol pyrophosphates. These are IPs characterized by containing one or more high-energy pyrophosphate moiety. PP-IPs were discovered in the early 1990's, in *Dictyostelium discoideum* (Europe-Finner et al., 1991, Mayr GW, 1992, Stephens et al., 1993), Entamoeba histolytica (Martin et al., 1993), and in mammalian cells (Menniti et al., 1993). The best-characterized member of this class is 5-diphosphoinositol pentakisphosphate (5-PP- P_5 or IP₇), which has five of the myo-inositol hydroxyls monophosphorylated, while the sixth, at the 5-position, contains a pyrophosphate group (Albert et al., 1997). The IP6K can also metabolize IP₅ to disphosphoinositol tetrakisphosphate (PP-IP₄) (Saiardi et al., 2000, Losito et al., 2009). Another isomer of IP₇, containing a pyrophosphate at the 1-position, can also be formed by a more recently identified enzyme termed diphosphoinositol pentakisphosphate kinase (PP-IP5K), though this enzyme appears to be predominantly associated physiologically with the formation of diphosphoinositol hexakisphosphate (PP₂-IP₄ or IP₈) (Choi *et al.*, 2007).

Among the many roles attributed to PP-IPs are the regulation of telomere length (Saiardi *et al.*, 2005, York *et al.*, 2005), DNA repair by homologous recombination (Luo *et al.*, 2002, Jadav *et al.*, 2013), response to hyperosmotic stress (Pesesse *et al.*, 2004, Choi *et al.*, 2007), vesicle trafficking (Saiardi *et al.*, 2000, Saiardi *et al.*, 2002), apoptosis (Morrison *et al.*, 2001, Nagata *et al.*, 2005), autophagy (Nagata *et al.*, 2010), binding of pleckstrin homology domains to phospholipids and proteins (Luo *et al.*, 2003, Gokhale *et al.*, 2013), transcription of glycolytic enzymes (Szijgyarto *et al.*,

2011), hemostasis (Ghosh *et al.*, 2013), phagocytic and bactericidal activities of neutrophils (Prasad *et al.*, 2011), epigenetic modifications to chromatin (Burton *et al.*, 2013) and exocytic insulin secretion (Illies *et al.*, 2007). PP-IPs may signal through allosteric interaction with proteins (i.e. binding to pleckstrin homology (PH) or other domains of proteins) or by phosphotransfer reactions (Saiardi, 2012, Shears, 2015, Wild *et al.*, 2016). The phosphotransfer reaction is non-enzymatic and requires a phospho-serine residue within an acidic region and consists in adding a second phosphate to the phosphor-serine resulting in pyrophosphorylation (Saiardi, 2012).

Trypanosoma brucei, which belongs to the group of parasites that causes African trypanosomiasis (sleeping sickness), possesses a PI-PLC that is stimulated by very low Ca²⁺ concentrations (King-Keller et al., 2015) and an IP₃ receptor that localizes to the acidocalcisomes instead of the endoplasmic reticulum (Huang et al., 2013). We now found that they also possess orthologs to IPMK, IP5K and IP6K, but do not have recognizable orthologs to PP-IP5K, inositol 1,4,5-trisphosphate 3-kinases (ITPKs) and inositol tetrakisphosphate 3-kinase 1 (ITPK1) (Table S1). The ortholog to IPMK (TbIPMK) was recently reported as essential for the bloodstream forms of the parasites (Cestari et al., 2015), suggesting that the soluble inositol phosphate pathway is essential for the parasite. The orthologs to IP5K and IP6K were not recognizable by sequence only and were wrongly annotated as a putative hypothetical protein and as inositol polyphosphate-like protein, respectively. In the present study, we thoroughly characterized the soluble inositol phosphate pathway of T. brucei. We cloned, expressed and biochemically characterized the recombinant enzymes from T. brucei, complemented yeast mutants to demonstrate their function, analyzed their products, studied the inositol phosphate metabolism of T. brucei cells, and revealed the link of this pathway to the synthesis of polyphosphate in acidocalcisomes.

Results

105

106

107

108

109

110

111

112

113

114

115

116

117

118

119

120

121

122

123

124

125

126

103

Gene homology searches followed by validation of their activity (see below) have allowed to identify in the T. brucei genome (http://www.tritrypdb.org/tritrypdb/) the presumably gene orthologs to the inositol phosphate kinases encoding inositol polyphosphate multikinase (IPMK in mammals, and Arg82p or Ipk2p in yeast) (Tb427tmp.211.3460); the IP₅ kinase (IPPK or IP5K in mammals, and Ipk1p in yeast) (Tb427.04.1050); and the IP₆ kinase (IP6K in mammals, and Kcs1p in yeast) (Tb427.07.4400), (Fig. 1), and named *TbIPMK*, *TbIP5K*, and *TbIP6K*, respectively (Table S1). No orthologs to diphosphoinositol pentakisphosphate kinase (PP-IP5K in mammals, or Vip1 in yeasts) were found, although orthologs to this gene are present in Apicomplexan (Laha et al., 2015) and Giardia (EuPathDB). The orthologs to TbIPMK, TbIP5K, and TbIP6K identified in T. cruzi (TcCLB.510741.110, TcCLB.506405.90, TcCLB.504213.90) and Leishmania major (LmjF.35.3140, LmjF.34.3700, LmjF.14.0340) shared 45%, 36%, 35%, and 29%, 28%, 24% amino acid identity, respectively. Those of T. brucei share 15%, 16%, and 15% identity with the human enzymes, respectively. Structural analyses (ELM and TMHMM servers) predicted no transmembrane domains. A signal peptide was predicted for TbIP5K, but not for TbIPMK or TbIP6K. Mature proteins of 342, 461, and 756 amino acids with predicted molecular weights of 38.8, 51, and 82.6 kDa, for TbIPMK, TbIP5K, and TbIP6K, respectively, were also predicted. Amino acids 138-147 of TbIPMK, and 588-596 of TbIP6K contained the conserved sequence PCVLDL(I)KL(M)G demonstrated previously as the putative inositol phosphate binding site that catalyzes the transfer of phosphate from ATP to inositol phosphates (Bertsch et al., 2000). TbIP5K possesses the sequence PVLDIELL (amino acids 269-276) instead. Both TbIPMK and TbIP6K have a SASLL or TSSLL domain present in most members of this family of enzymes and required for enzymatic activity (Saiardi et al., 2001b, Nalaskowski et al., 2002).

We utilized homologous recombination to add a hemagglutinin (HA) or c-Myc tag to the endogenous loci (Oberholzer *et al.*, 2006) of TbIPMK, TbIP5K and TbIP6K. All three inositol phosphate kinases are expressed in procyclic forms (PCF) of *T. brucei* (Fig. 2A). Although the predicted MW of TbIP6K is 82.6 kDa the enzyme has multiple phosphorylations (Urbaniak *et al.*, 2013) and these post-translational modifications (in addition to the HA tag) could result in a higher apparent MW. Interestingly, TbIP5K revealed no expression when using the HA-tag, but a protein with the expected size was detected when using a c-Myc tag (Fig. 2A). In addition, we tagged the three IP kinases in *T. brucei* bloodstream forms (BSF) but no clear bands were detected by western blot analyses although the tagged genes were expressed at the mRNA level (data not shown), suggesting that protein expression is lower in BSF than in PCF.

Characterization of the inositol phosphate multikinase (TbIPMK)

To characterize the enzymatic activity of TbIPMK we expressed it as fusion protein with an *N*-terminal polyhistidine tag, purified and tested its activity *in vitro*. We found that it catalyzes the formation of IP₅ from IP₃ or IP₄, as detected by polyacrylamide gel electrophoresis (Fig. 2B). Inositol-1,4,5-trisphosphate (I(1,4,5)P₃) but not inositol-1,3,4-trisphosphate (I(1,3,4)P₃) could be used as substrate while both inositol-1,3,4,5-tetraphosphate (I(1,3,4,5)P₄) and inositol-1,4,5,6-tetraphosphate (I(1,4,5,6)P₄) could be used for the generation of inositol-1,3,4,5,6-pentakisphosphate (I(1,3,4,5,6)P₅) (Fig. 2B), indicating that TbIPMK has a dual 3-kinase/6-kinase activity. An additional product, which runs closely but not identically to IP₆, was also detected when IP₃, IP₄, or IP₅ was used as substrate (Figs. 2B and 2C). The ability of IPMK to form PP-IP₄, an inositol pyrophosphate containing 6 phosphates and thus migrating closely to IP₆, has been demonstrated for the mammalian and yeast ortholog (Saiardi *et al.*, 2001a, Zhang *et al.*, 2001), and we therefore suspected that TbIPMK could have the same activity. A treatment with perchloric acid (PA), which degrades high-energy

phosphoanhydride bonds (pyrophosphates) and is inactive against the phosphoester bond of IP₆ (Fig. 2C) (Pisani *et al.*, 2014), demonstrated that the highly phosphorylated product of TbIPMK is a pyrophosphate containing species, therefore PP-IP₄. The pH optimum of rTbIPMK was determined. TbIPMK has the maximum activity for IP₃ at the pH range of 6.5-7.0 (Fig. 2D). We also tested the ability of TbIPMK to phosphorylate different isomers of IP₅. Recombinant TbIPMK was able to phosphorylate I(1,2,4,5,6)P₅ and I(1,2,3,4,5)P₅ to IP₆ after short incubation times, but it was not able to use I(2,3,4,5,6)P₅, I(1,3,4,5,6)P₅, (I(1,2,3,5,6)P₅, or (I(1,2,3,4,6)P₅ as substrate (Fig. 2E). Although I(1,2,4,5,6)P₅ and I(1,2,3,4,5)P₅ would not be physiological substrates, the results again confirms a 3/6-kinase activity. Interestingly, TbIPMK could also phosphorylate I(1,4)P₂ to IP₄ (Fig. 2B). The mammalian IPMK has been reported to have PI3-kinase activity that produces PIP₃ from PIP₂ (Resnick *et al.*, 2005). However, our in vitro activity tests using PIP₂ as substrate revealed no such activity (data not shown) in agreement with the results of a previous report (Cestari *et al.*, 2016).

The ability of TbIPMK to act on IP₃ in vivo was tested by complementation of a null mutant for its ortholog ARG82 ($arg82\Delta$ in Saccharomyces cerevisiae. Fig. 3A shows the HPLC analysis of soluble inositol phosphates isolated from yeast labeled with [3 H]inositol. Arg82p phosphorylates IP₃ to produce IP₄ and IP₅, and in its absence there is accumulation of IP₃, instead of the accumulation of IP₆ that occurs in wild type yeast (Fig. 3A). The metabolic pathway from IP₃ to IP₆ was restored by complementation with TbIPMK (Fig. 3A). These results indicate that TbIPMK function as part of the IP₆ biosynthetic pathway established in yeast (York et al., 1999). We also examined the ability of TbIPMK to rescue the growth defect of $arg82\Delta$ yeast. Complementation of $arg82\Delta$ with TbIPMK rescued their growth defect (Fig. 3B, and 3C). Therefore, TbIPMK was able to complement yeast deficient in its ortholog Arg82p, providing molecular evidence of its function. The results also suggest that the pathway for IP₅ synthesis is similar to that present in yeast with conversion of I(1,4,5)P₃ into I(1,4,5,6)P₄ and I(1,3,4,5,6)P₅, TbIPMK acting as a 3 6-kinase. This is different from the pathway for

synthesis of $I(1,3,4,5,6)P_5$ present in humans, where the major activity of IP_4 kinase is phosphorylation at the D-5 position (Chang *et al.*, 2002).

178

176

177

Characterization of the inositol pentakisphosphate kinase (TbIP5K)

180

181

182

183

184

185

186

187

188

189

190

191

192

193

194

195

179

Although expression of polyhistidine-tagged TbIP5K was obtained in bacteria and the recombinant protein had the expected molecular mass, we were not able to detect its activity in vitro, even in the presence of different isomers of IP₅ (data not shown) suggesting that additional post-translational modifications are needed. In this regard, activity of human IP5K could only be obtained when expressed in insect cells (Verbsky et al., 2002). However, TbIP5K was able to complement null mutant yeast deficient in its ortholog IPK1 ($Ipk1\Delta$) (Fig. 3D). Ipk1p phosphorylates IP₅ to produce IP₆, and in its absence there is accumulation of IP5, instead of the accumulation of IP6 that occurs in wild type yeast. The metabolic pathway from IP₅ to IP₆ was restored by complementation with *TbIP5K* (Fig. 3D). The presence of a shoulder close to the PP-IP₄ eluting peak in the mutant yeast suggests the existence of two isomeric PP-IP₄ species. We also complemented yeast mutants for both $ipkl\Delta$ (IP5K) and kcs1\Delta (IP6K). These mutants accumulate IP2, IP3, IP4, and IP5 but no PP-IPs. While complementation with either TbIPMK or TbIP6K (not shown) alone did not change appreciably the inositol polyphosphate profile, synthesis of IP₆ was restored by complementation with *TbIP5K* alone (Fig. 3E), demonstrating that TbIP5K is the only inositol phosphate kinase identified in T. brucei genome that can produce IP₆.

196

Characterization of the inositol hexakisphosphate kinase (TbIP6K)

198

TbIP6K catalyzes the formation of IP₇ from IP₆. *TbIP6K* was also tagged with an HA tag using homologous recombination with the endogenous gene loci (Oberholzer *et al.*, 2006). We detected expression of the enzyme in *T. brucei* procyclic forms (PCF) by western blot analysis (Fig. 2A). Recombinant TbIP6K was found to generate PP-IP₄ from IP₅ and IP₇ from IP₆ (Fig. 4A). Interestingly TbIP6K was not able to generate IP₈ using a 5PP-IP₇ as substrate, which suggests that, as IP6K from yeast and mammals, TbIP6K phosphorylates phosphate position D-5. Therefore, TbIP6K is able to generate two PP-IPs *in vitro*: PP-IP₄, and IP₇. The activity of TbIP6K was tested *in vivo* by complementation of a *null* mutant for its IP6K ortholog (*KCS1*) in *S. cerevisiae*. In the absence of *KCS1* there is no accumulation of IP₇, but the metabolic pathway from IP₆ to IP₇ is restored by complementation with *TbIP6K* (Fig. 4B). Complementation of *Kcs1*Δ *TbIP6K* also rescued the growth defect of these mutants (Fig. 4C and 4D). The TbIP6K enzymatic activity has optimum pH 6.0-7.0 (Fig. 4E).

Characterization of inositol phosphates from T. brucei cells

Previous attempts to characterize soluble inositol phosphates from *T. brucei* (Moreno *et al.*, 1992) and *T. cruzi* (Docampo *et al.*, 1991) only detected IP, IP₂ and IP₃. We used increased labeling time to 40 hours (BSF) and 75 hours (PCF) with [³H]inositol and used an improved protocol for purifying and analyzing inositol phosphates (see Materials and methods). Using these conditions, we were able to detect a small peak of IP₆ in PCF but not in BSF of the parasite (Figs. 5A, and 5B). The inability to detect radiolabeled IP₆ in the BSF might simply reflect the lower number of cells that can be obtained in culture. To improve the detection of IP₆ we used a different approach that does not require metabolic labeling with [³H]inositol. We extracted IPs from large amounts of cells (see Materials and methods) and assayed extracts by 35% polyacrylamide gel electrophoresis (PAGE). A band that runs like the IP₆ standard and that disappears after treatment of the extracts with phytase (Phy) was

observed in both PCF and BSF (Figs. 5C, and 5D). Other highly phosphorylated inositol phosphates were not detected. These results confirm that both PCF and BSF TbIPMK and TbIP5K can sequentially synthesize IP₆ in *T. brucei*.

227

224

225

226

Biological relevance of the TbIPMK pathway

229

230

231

232

233

234

235

236

237

238

239

240

241

242

243

244

245

246

247

228

Yeast lacking Arg82p have no observable inorganic polyphosphate accumulation (Lonetti et al., 2011). As polyphosphate has important roles in trypanosomes, including growth, response to osmotic stress, and maintenance of persistent infections (Lander et al., 2016), we investigated whether deletion of soluble inositol polyphosphates affected the levels of polyphosphate in T. brucei. We used the TbIPMK conditional knockout BSF cell line previously described (Cestari et al., 2015). Removal of tetracycline to induce the knockdown of TbIPMK dramatically reduced its expression more than 100fold (Fig. 6A). Growth stalled after the first day without tetracycline (Fig. 6B). A resulting progressive reduction in polyphosphate levels was detected (Fig. 6C). Acidocalcisomes are the main cellular storage compartment for polyphosphate in trypanosomes (Lander et al., 2016). However, examination of the cells by super-resolution microscopy with antibodies against the vacuolar proton pyrophosphatase (TbVP1) showed no apparent difference in labeling or distribution of acidocalcisomes between control and TbIPMK mutant cells (Figure S1). In previous work we demonstrated that a knockdown of the TbVtc4, which catalyzes the synthesis and translocation of polyphosphate into acidocalcisomes, results in less electron-dense organelles, as examined by electron microscopy (Ulrich et al., 2014). We hypothesized that if the polyphosphate reduction observed (Fig. 6C) was primarily within acidocalcisomes, we should observe similar changes in the *TbIPMK* mutant cells. Indeed, electron microscopy of the *TbIPMK* mutants showed a reduction in the number (Fig. 6D), size, and electron density (compare Fig. 6E and 6F) of electron-dense organelles identifiable as

acidocalcisomes. This result indicates that acidocalcisome polyphosphate synthesis is disrupted by ablation of the inositol phosphate signaling pathway.

250

248

249

Discussion

252

253

254

255

256

257

258

259

260

261

262

263

264

265

266

267

268

269

270

271

272

251

Our work establishes the presence of an inositol pyrophosphate (PP-IPs) synthesis pathway in T. brucei. We demonstrated that genes encoding proteins with homology to kinases involved in the generation of IP₅ from IP₄ and IP₃ (TbIPMK), of IP₆ from IP₅ (TbIP5K), and of IP₇ from IP₆ (TbIP6K) are present in the *T. brucei* genome (*TbIPMK*, *TbIP5K*, and *TbIP6K*). To demonstrate that these genes encode for functional enzymes we complemented yeast strains deficient in their corresponding orthologs and compared their products with those produced in the wild type strain providing in vivo genetic evidence of their function. We did not compare them with the knockout strains overexpressing the endogenous genes because the heterologous gene expression is often hampered by a diverse genetic code usage and by the lack of yeast specific post-translational processing. Thus, the heterologous genes are regularly expressed from a stronger promoter. The overexpressing of the endogenous gene from a stronger promoter might generate, to the contrary, 'hyper' phenotype and not a normal WT phenotype and our aim was to demonstrate their function and not to compare their activities to those of the overexpressed endogenous genes. Suppression of this pathway in T. brucei BSF resulted in a significant decrease in polyphosphate levels and in morphological alterations of the acidocalcisomes. The results suggest that this pathway is important for polyphosphate synthesis in acidocalcisomes. Examination of the protein sequences of TbIPMK, TbIP5K, and TbIP6K indicated low identity with the mammalian enzymes but conservation of the putative binding site that catalyzes the transfer of phosphate from ATP to IPs, as well as of other domains required for enzymatic activity. The

expression of these three kinases is very low in BSF since no clear bands were detected by western

blot analyses of endogenous tagged lines, although gene expression is detectable at the mRNA level. Conversely, all three kinases can be easily identified by western blot analysis of PCF. Our results suggest, in agreement with the presence of these enzymes in other unicellular organisms such as *D. discoideum* (Europe-Finner *et al.*, 1991, Mayr GW, 1992, Stephens *et al.*, 1993), and *E. histolytica* (Martin *et al.*, 1993), an early emergence of this pathway preceding the origin of multicellularity.

The application of polyacrylamide gel electrophoresis (PAGE) and toluidine blue staining (Losito *et al.*, 2009, Pisani *et al.*, 2014) allowed the characterization of the IPs synthesizing kinases of *T. brucei* and the identification of the products of each reaction bypassing the need for extraction under the strong acidic conditions required for HPLC analysis that has been shown to degrade some of the most highly phosphorylated species (Losito *et al.*, 2009).

Previous work has indicated that TbIPMK is essential for growth (Cestari et al., 2015) and infectivity (Cestari et al., 2016) of T. brucei BSF, and partially characterized the recombinant enzyme (Cestari et al., 2016). We confirmed that TbIPMK prefers I(1,4,5)P₃ and I(1,3,4,5)P₄ as substrates (Cestari et al., 2016) and found that it does not phosphorylate I(1,3,4)P₃. We also confirmed that TbIPMK cannot phosphorylate the lipid PIP₂ to PIP₃ (Cestari et al., 2016), as the human enzyme does (Resnick et al., 2005). In addition, we found that the enzyme can use I(1,3,4,5)P₄ and I(1,4,5,6)P₄ for the generation of $I(1,3,4,5,6)P_5$ indicating that TbIPMK has a dual 3-kinase/6-kinase activity. This is in contrast to the human enzyme, where the major activity of IP₄ kinase is phosphorylation at the D-5 position (Chang et al., 2002). Moreover, we demonstrated that TbIPMK is able to generate PP-IP₄ in vitro, using either $I(1,4,5)P_3$, $I(1,3,4,5)P_4$ or $I(1,3,4,5,6)P_5$, as well as IP_6 from $I(1,2,4,5,6)P_5$, or (I(1,2,3,4,5)P₅ as substrate, again indicating a 3/6-kinase activity. TbIPMK has a neutral pH optimum for phosphorylation of both IP₃ and IP₄. Previous work (Cestari et al., 2016) described inhibitors of this enzyme that inhibited T. brucei BSF growth. However, their IC50s against the enzymes were higher (3.4-5.33 µM) than the EC₅₀s for their growth inhibition (0.51-0.83 µM), suggesting that either the drugs are accumulated or other targets might be involved in the sensitivity of T. brucei BSF to

those inhibitors. The search for more specific inhibitors is warranted to demonstrate the relevance of this pathway to human disease and drug therapy. Interestingly, a recombinant multi-domain protein from *Plasmodium knowlesi* termed PkIPK1 was shown to have IPMK-like activity and was able to generate I(1,3,4,5)P₄ from I(1,4,5)P₃ and I(1,2,4,5,6)P₅ from either I(1,2,5,6)P₄ or I(1,3,4,6)P₄, showing 3/5-kinase activity (Stritzke *et al.*, 2012).

We were not able to detect activity of the recombinant IP5K in the presence of different isomers of IP₅ suggesting that, as proposed for the mammalian enzyme, post-translational modifications are needed for its activity (Verbsky *et al.*, 2002). However, TbIP5K was able to complement *null* mutant yeast deficient in its ortholog IPK1 ($Ipk1\Delta$), providing genetic evidence of its function.

Recombinant TbIP6K was able to generate PP-IP₄ from IP₅ and IP₇ from IP₆, but was not able to generate IP₈ using a 5-PP-IP₅ as substrate suggesting that, as IP6K from mammalian cells (Draskovic *et al.*, 2008), TbIP6K phosphorylates phosphate at position D-5. Therefore, TbIP6K is able to generate two PP-IPs in vitro: PP-IP₄, and IP₇. Complementation of yeast deficient in its ortholog confirmed the function of this enzyme.

T. brucei incorporates poorly the radioactive tracer [³H]inositol a feature previously observed in Dictyostelium discoideum (Losito et al., 2009). Nevertheless, improved metabolic labeling with [³H]inositol resulted in detection of IP, IP₂, IP₃ and IP₆ by HPLC analysis of PCF extracts. In contrast to the results obtained using similar methods in yeasts (Azevedo et al., 2006), plants (Phillippy et al., 2015) or animal cells (Guse et al., 1993), only very low levels of IP₆ were detected and no labeled IP₆ was detected by HPLC using BSF extracts. However, IP₆ was clearly detected by PAGE and toluidine blue staining when large numbers of parasites were used. No inositol pyrophosphates were detected since to purify and visualize IPs we removed the abundant inorganic polyphosphate (polyP) by acidic treatment, procedure that would degrade IP₇ to IP₆. However, the absence of IP₇ could be also attributed to the high turnover of these important signaling molecules (Glennon et al., 1993, Burton et al., 2009). Some cells accumulate IP₆ and produce IP₇ upon signaling events. For instance,

Cryptococcus neoformans requires synthesis of IP₇ for successful establishment of infection (Li et al., 2016). A recent study demonstrated that IP₇ binds the SPX domain of proteins involved in phosphate homeostasis in plants, yeast and humans with high affinity and specificity and postulated the role of this domain as a polyphosphate sensor domain (Wild et al., 2016, Azevedo et al., 2017). Two proteins in T. brucei possess SPX domains, TbVtc4 (Lander et al., 2013), which is involved in polyphosphate synthesis and translocation, and TbPho91 (Huang et al., 2014), a phosphate transporter. Both proteins localize to acidocalcisomes (Huang et al., 2014), the main polyphosphate storage of these cells. Our results, showing lower levels of polyphosphate and altered acidocalcisomes in TbIPMK BSF mutants, support the link between PP-IPs and polyphosphate metabolism.

In summary, both recombinant enzymes, TbIPMK and TbIP6K, are able to generate inositol pyrophosphates. The essentiality of the first enzyme of this pathway, TbIPMK, for growth and infectivity of *T. brucei* BSF (Cestari *et al.*, 2015, Cestari *et al.*, 2016) suggests that the study of the PP-IPs pathway in trypanosomes could lead to the elucidation of potentially multiple important roles of these compounds, possibly linked to the synthesis of polyphosphate. Differences between mammalian and trypanosome metabolism of these compounds could provide potential targets for drug development.

Experimental procedures

Chemicals and reagents

Mouse antibodies against HA were from Covance (Hollywood, FL). Inositol, myo-[1,2-3H(N)] (30-80 Ci/mmol, ART 0261A) was from American Radiolabeled Chemicals, Inc. Goat anti-mouse antibodies were from LI-COR Biosciences (Lincoln, NE). Laemmli sample buffer was from Bio-Rad Laboratories (Hercules, CA). The bicinchoninic (BCA) protein assay kit was from Pierce (Thermo

Fisher Scientific, USA). Titanium dioxide (TiO₂) beads (Titansphere ToO 5 μm) were from GL Sciences (USA). PrimeSTAR HS DNA polymerase was from Clontech Laboratories Inc. (Takara, Mountain View, CA). Vector pET32 Ek/LIC was from Novagen (Merck KGaA, Darmstadt, Germany). Acrylamide mix was from National Diagnostics (Chapel Hill, NC). CelLytic M cell lysis reagent, P8340 protease inhibitor, protease inhibitors, Benzonase Nuclease, antibody against c-Myc, inositol phosphates, and other analytical reagents were from Sigma-Aldrich (St. Louis, MO).

Cell cultures

T. brucei Lister strain 427 BSF and PCF were used. The BSF were cultivated at 37°C in HMI-9 medium (Hirumi *et al.*, 1989) supplemented with 10% heat inactivated fetal bovine serum (FBS, Sigma). The PCF were cultivated at 28°C in SDM-79 medium (Cunningham, 1977) supplemented with 10% heat-inactivated FBS and hemin (7.5 μg/ml). To determine the presence of IP₆ by PAGE analysis *T. brucei* BSF were also isolated from infected mice (Balb/c, female, 6-8 weeks old) and rats (Wistar, male retired breeders), as described previously (Cross, 1975). *T. brucei IPMK* conditional knockout cell line was obtained and grown as described previously (Cestari *et al.*, 2015).

Yeast strains

The yeast strains used in this study are isogenic to DDY1810 (MATa leu2-3,112 trp1- Δ 901 ura3-52 prb1-1122 pep4-3 prc1-407), except for the $ipk1\Delta kcs1\Delta$ strain that is isogenic to BY4741 (MATa his3 Δ 1 leu2 Δ 0 met15 Δ 0 ura3 Δ 0) and was previously described (Saiardi *et al.*, 2002). The DDY1810 protease deficient strain is often used to increase the expression of exogenous proteins upon overexpression due to a deletion on the Pep4 protease. The generation of DDY1810 $kcs1\Delta$ strain was

previously described (Onnebo *et al.*, 2009). The $arg82\Delta$, $ipk1\Delta$ yeast strains in the DDY1810 genetic background were generated following standard homologous recombination techniques (Gueldener *et al.*, 2002) using oligonucleotides listed in Table S2. Initially diagnostic PCR was performed to confirm the correct integration of the deletion constructs. Subsequently, the soluble inositol polyphosphate profile of these new strains was used to phenotypically validate the correct homologous recombination event.

378

372

373

374

375

376

377

Epitope tagging, cloning expression and biochemical characterization of inositol phosphate kinases

380

381

382

383

384

385

386

387

388

389

390

391

392

393

394

395

396

379

We followed a one-step epitope-tagging method (Oberholzer et al., 2006) to produce the C-terminal HA- or cMyc-tagging cassettes for transfection of T. brucei PCF (Table S2). Briefly, the tagging cassettes containing selection markers were generated for cell transfection by PCR using pMOTag4H and pMOTag33M as templates with the corresponding PCR primers of the genes (Table S2). Transfection was performed using 2.5 x 10⁷ PCF parasites from log phase. Cells were harvested at 1,000 x g for 10 min, washed with 10 ml of ice-cold sterile Cytomix buffer (2 mM EGTA, 3 mM MgCl₂, 120 mM KCl, 0.5% glucose, 0.15 mM CaCl₂, 0.1 mg/ml bovine serum albumin, 10 mM K₂HPO₄/KH₂PO₄, 1 mM hypoxanthine, 25 mM Hepes, pH 7.6), centrifuged at 1,000 x g for 7 min, suspended in 0.5 ml Cytomix and transferred to an ice-cold 4 mm gap cuvette (Bio-Rad) containing 15 µg of PCR amplicon. Cuvettes were incubated 5 min on ice and immediately electroporated twice in Bio-Rad GenePulser XcellTM Electroporation System at 1.5 kV, 25 µF. Cuvettes were kept on ice for one minute between electroporation pulses. Cell mixture was transferred to SDM-79 medium with 15% FBS. After 6 h appropriate antibiotics were added. The sequences of the three kinases *TbIPMK*, TbIP5K and TbIP6K were amplified from genomic DNA by PCR (Table S2) using PrimeSTAR HS DNA polymerase and cloned into ligation independent expression vector pET32 Ek/LIC, as recommended by the manufacturer. Constructs were cloned into Escherichia coli BL21CodonPlus(DE3) and protein expression was induced with 1 mM isopropyl β-D-1-thiogalactopyranoside (IPTG) in Luria Bertani broth for 3 h. Protein purification was performed using affinity chromatography HIS-Select® Cartridge, according to the manufacturer's instructions. We tested activity of the kinases on commercially available substrates. Enzyme assays were performed at 37°C using approximately 50 ng of recombinant protein, 20 mM Hepes buffer, pH 7.0, 0.2-0.5 mM substrate, 6 mM MgCl₂, 100 mM NaCl, 1 mM dithiotreitol (DTT), 0.5 mM ATP, 10 mM phosphocreatine, and 40 U creatine kinase. Enzymatic reactions were stopped with 3 μl of 100 mM EDTA and kept on ice or frozen until further use. Reaction products were resolved by PAGE using 35% acrylamide/bis-acrylamide 19:1 gels in Tris/Borate/EDTA (TBE) buffer as described by (Losito et al., 2009). Gels were stained with toluidine blue (Losito et al., 2009).

RNA quantification

The *TbIPMK* conditional knockout cell line was grown with or without 1 μg/ml tetracycline and harvested at room temperature. RNA was extracted with TRI reagent (Sigma) and used as template for cDNA synthesis with SuperScript III RNA Polymerase (ThermoFisher) and oligo-dT as recommended by the manufacturer. We then performed qRT-PCR analysis using specific primers (Table S2) and SYBR Green Supermix (Bio-Rad). Relative *TbIPMK* gene expression relative to actin was calculated using CFX ManagerTM Software (Bio-Rad).

Western blot analyses

Cells were harvested, washed twice in PBS, and lysed with CelLytic M cell lysis reagent containing protease inhibitor cocktail (Sigma P8340) diluted 1:250, 1 mM EDTA, 1 mM phenylmethanesulfonyl fluoride (PMSF), 20 µM *trans*-epoxysuccinyl-L-leucylamido(4-guanidino)butane (E64) and 50 U/ml

Benzonase Nuclease (Millipore). The protein concentration was determined by using a BCA protein assay kit. The total cell lysates were mixed with 2X Laemmli sample buffer at 1:1 ratio (vol/vol) and directly loaded in 10% SDS-PAGE. The separated proteins were transferred onto nitrocellulose membranes using a Bio-Rad transblot apparatus. The membranes were blocked with 5% (wt/vol) nonfat milk in PBS containing 0.5% Tween-20 (PBS-T) at 4°C overnight. The blots were incubated for 1 hour with mouse antibodies against HA (1:1000) or mouse antibodies against c-Myc (1:1000). After five washings with PBS-T the blots were incubated with goat anti-mouse antibodies at a dilution of 1:15000 and developed using an Odyssey CLx Infrared Imaging System (LI-COR) according to the manufacturer instructions.

Yeast complementation

S. cerevisiae strains generated from DDY1810 were used: arg82Δ, ipk1Δ, kcs1Δ, ipk1Δkcs1Δ. TbIPMK, TbIP5K and TbIP6K were amplified from T. brucei Lister 427, cloned into plasmid pADH:GST (pYES-ADH1-GST) (Azevedo et al., 2009). Yeast cells were grown for 48 h in CSM plates. One colony was collected and suspended in 0.2 M lithium acetate with 25% polyethylene glycol solution and 0.1 M DTT. Cells were homogenized in 100 μl of solution with 100 ng of plasmid DNA and 5 μl of salmon sperm (Sigma D76560). Cells were incubated at 42°C for 30 min and immediately plated in CSM -URA plates. Colonies were used for further experiments.

Titanium dioxide bead extraction

We adapted the method of Wilson et al. (Wilson *et al.*, 2015) for cell extraction of inositol polyphosphates. Cells (5 x 10⁹) were harvested and washed twice in washing buffer A with glucose (BAG, 116 mM NaCl, 5.4 mM KCl, 0.8 mM MgSO₄, 50 mM Hepes, ph 7.3, and 5.5 mM glucose).

The pellet was then mixed with 1 M perchloric acid, resuspended by sonication (40% amplitude) for 10 s and kept at room temperature for 15 min. The sample was centrifuged art 18,000 x g for 5 min and the supernatant was transferred to a new tube and boiled for 30 min to remove the large amount of polyphosphate present in T. brucei. Seven mg of TiO_2 beads were washed with water and 1 M perchloric acid, and added to the sample and left rotating for 30 min. Beads were centrifuged at 3,500 x g and inositol phosphates eluted with 1 M KOH, 10 mM EDTA. The sample was neutralized with perchloric acid and split into two. One half was digested with phytase (0.1 mg/ml) in the same medium at pH $5.0 \text{ and } 37^{\circ}\text{C}$ for 1 h. Extracts were resolved by 35% PAGE analysis as described above.

HPLC analysis

Inositol phosphate analysis was performed according to (Azevedo *et al.*, 2006). Briefly, yeast liquid cultures were diluted to OD₆₀₀ 0.005 in inositol free media supplemented with 5 μCi/ml [³H] inositol and grown overnight at 30°C with shaking. Cells were washed twice with water and immediately incubated with ice-cold 1 M perchloric acid and 3 mM EDTA. Glass beads were added and cells lysed by vortexing at 4°C for 2 min, 3 times. Lysates were centrifuged and supernatants neutralized with 1 M K₂CO₃ and 3 mM EDTA. Samples were analyzed by strong anion exchange HPLC using SAX 4.6125 mm column (Whatman cat. no. 4621-0505). The column was eluted with two slightly different gradients generated by mixing buffer A (1 mM Na₂EDTA) and buffer B [buffer A plus 1.3 M (NH₄)₂HPO₄ (pH 3.8 with H₃PO₄)] as follows: 0–5 min, 0% B; 5–10 min, 0–30% B; 10–60 min, 30–100% B; 60–80 min, 100% B; or as follow: 0–5 min, 0% B; 5–10 min, 0–10% B; 10–85 min, 20–100% B; 85–100 min 100% B. Four mL of Ultima-Flo AP liquid scintillation cocktail (Perkin-Elmer cat. no. 6013599) was added to each fraction, mixed and radioactivity quantified in a scintillation counter.

T. brucei PCF (~3x10⁶ cells) were labeled with 5 μ Ci/ml of 1,2-[³H]-inositol in SDM-79 medium (with 10% FBS) and grown for approximately 72 h. *T. brucei* BSF (~2x10⁵ cells) were labeled with 5 μ Ci/ml of 1,2-[³H]-inositol in HMI-9 medium (with 10% FBS) and grown for approximately 40 h. Cells were washed with PBS or BAG twice and frozen immediately. Soluble inositol phosphates were extracted and analyzed as described before (Azevedo *et al.*, 2006), with minor modifications. Briefly, cells were suspended in ice-cold perchloric acid and broken by vortexing for 2 min. All steps were performed at 4°C. Lysates were centrifuged for 5 min at 18,000 x g and supernatants transferred to new tubes, where the pH was neutralized with 1 M K₂CO₃ and 3 mM EDTA. Samples were stored at 4°C and resolved by HPLC.

Polyphosphate extraction and measurement

Short chain polyphosphate was extracted from BSF *T. brucei* and quantified as described previously (Ulrich *et al.*, 2014).

- 489 Immunofluorescence Assay
 - T. brucei BSF were washed with BAG and fixed with 2% paraformaldehyde in BAG for 1 h at room temperature. Then they were adhered to poly-L-lysine coated coverslips and permeabilized with 0.1% Triton X-100 in PBS for 5 min. Blocking was performed overnight at 4°C in PBS containing 100 mM NH₄Cl, 3% BSA, 1% fish gelatin and 5% goat serum. Cells were then incubated with anti-TbVP1 polyclonal Guinea pig antibody (1:100) for 1 h and subsequently with Alexa 488-conjugated goat anti-Guinea pig antibody (1:1000) for 1h. Microscopy images were taken with a 100X oil immersion objective, a high-power solid-state 405 nm laser and EM-CCD camera (Andor iXon) under

nonsaturating conditions in a Zeiss ELYRA S1 (SR-SIM) super resolution microscope. Images were acquired and processed with ZEN 2011 software with SIM analysis module.

Electron microscopy

Imaging of whole *T. brucei* BSF and determination of morphometric parameters were done as described previously (Ulrich *et al.*, 2014).

Statistical analysis

All experiments were repeated at least three times (biological replicates) with several technical replicates as indicated in the figure legends, and where indicated results are expressed as means \pm s.d. or s.e.m. of n experiments. Statistical analyses were performed using the Student's t-test. Results are considered significant when P < 0.05.

Acknowledgments

We thank Noelia Lander for help with pET32 cloning, Thomas Seebeck for the pMOTag vectors, Igor Cestari and Ken Stuart for the *TbIPMK* conditional knockout cell line, Muthugapatti Kandasamy and the Biomedical Microscopy Core of the University of Georgia for help with the super-resolution microscope, and John Shields and Mary Ard from the Georgia Electron Microscopy for help with electron microscopy. This work was funded by U.S. National Institutes of Health (grant AI1077538) and supported by the Medical Research Council (MRC) core support to the MRC/UCL Laboratory for Molecular Cell Biology University Unit (MC_UU_1201814). C.C was partially supported by an European Molecular Biology Organization (EMBO) Short Term Fellowship and Center for Tropical and Emerging Global Diseases (CTEGD) travel fellowship.

522	Competing interests
523	The authors declare no competing or financial interests
524	
525	Author contributions
526	C.C., A.S. and R.D. designed the experiments and analyzed the data. C.C. and A.S. conducted the
527	experiments. R.D. wrote the majority of the manuscript, with specific sections contributed by C.C.,
528	and A.S. R.D. and A.S. supervised the work and contributed to the analysis of experiments.
529	
530	Supporting information
531	Supplementary information available online at:
532	
533	Abbreviated Summary
534	The work identifies the enzymes involved in the inositol pyrophosphate synthesis pathway in
535	Trypanosoma brucei and establishes a link between this pathway and the synthesis of polyphosphate
536	in acidocalcisomes.
537	
538	References
539	
5 40	
540	Albert, C., Safrany, S.T., Bembenek, M.E., Reddy, K.M., Reddy, K., Falck, J., et al. (1997).
541	Biological variability in the structures of diphosphoinositol polyphosphates in <i>Dictyostelium</i>
542	discoideum and mammalian cells. Biochem J 327: 553-560.
543	Azevedo, C., Burton, A., Ruiz-Mateos, E., Marsh, M. and Saiardi, A. (2009). Inositol pyrophosphate
544	mediated pyrophosphorylation of AP3B1 regulates HIV-1 Gag release. Proc Nat Acad Sci USA
545	106: 21161-21166.

- Azevedo, C. and Saiardi, A. (2006). Extraction and analysis of soluble inositol polyphosphates from
- yeast. *Nat Prot* **1:** 2416-2422.
- Azevedo, C. and Saiardi, A. (2017). Eukaryotic Phosphate Homeostasis: The Inositol Pyrophosphate
- Perspective. *Trends Biochem Sci* **42:** 219-231.
- Berridge, M.J. (2009). Inositol trisphosphate and calcium signalling mechanisms. Biochim Biophys
- 551 *Acta* **1793:** 933-940.
- Bertsch, U., Deschermeier, C., Fanick, W., Girkontaite, I., Hillemeier, K., Johnen, H., et al. (2000).
- The second messenger binding site of inositol 1,4,5-trisphosphate 3-kinase is centered in the
- catalytic domain and related to the inositol trisphosphate receptor site. *j Biol Chem* **275:** 1557-
- 555 1564.
- Burton, A., Azevedo, C., Andreassi, C., Riccio, A. and Saiardi, A. (2013). Inositol pyrophosphates
- regulate JMJD2C-dependent histone demethylation. *Proc Nat Acad Sci USA* **110:** 18970-18975.
- Burton, A., Hu, X. and Saiardi, A. (2009). Are inositol pyrophosphates signalling molecules? J Cell
- 559 *Physiol* **220**: 8-15.
- 560 Cestari, I., Haas, P., Moretti, N.S., Schenkman, S. and Stuart, K. (2016). Chemogenetic
- characterization of inositol ophosphate metabolic pathway reveals druggable enzymes for
- targeting kinetoplastid parasites. *Cell Chem Biol* **23:** 608-617.
- 563 Cestari, I. and Stuart, K. (2015). Inositol phosphate pathway controls transcription of telomeric
- expression sites in trypanosomes. *Proc Nat Acad Sci USA* **112:** E2803-2812.
- Chang, S.C., Miller, A.L., Feng, Y., Wente, S.R. and Majerus, P.W. (2002). The human homolog of
- the rat inositol phosphate multikinase is an inositol 1,3,4,6-tetrakisphosphate 5-kinase. J Biol
- 567 *Chem* **277:** 43836-43843.
- 568 Choi, J.H., Williams, J., Cho, J., Falck, J.R. and Shears, S.B. (2007). Purification, sequencing, and
- molecular identification of a mammalian PP-InsP5 kinase that is activated when cells are
- exposed to hyperosmotic stress. *J Biol Chem* **282**: 30763-30775.

- 571 Cocco, L., Follo, M.Y., Manzoli, L. and Suh, P.G. (2015). Phosphoinositide-specific phospholipase C
- in health and disease. *J Lipid Res* **56:** 1853-1860.
- 573 Cross, G.A. (1975). Identification, purification and properties of clone-specific glycoprotein antigens
- 574 constituting the surface coat of *Trypanosoma brucei*. *Parasitology* **71:** 393-417.
- 575 Cunningham, I. (1977). New culture medium for maintenance of tsetse tissues and growth of
- trypanosomatids. *J Protozool* **24:** 325-329.
- 577 Docampo, R. and Pignataro, O.P. (1991). The inositol phosphate/diacylglycerol signalling pathway in
- 578 *Trypanosoma cruzi. Biochem J* **275:** 407-411.
- 579 Draskovic, P., Saiardi, A., Bhandari, R., Burton, A., Ilc, G., Kovacevic, M., et al. (2008). Inositol
- hexakisphosphate kinase products contain diphosphate and triphosphate groups. *Chem Biol* **15**:
- 581 274-286.
- Europe-Finner, G.N., Gammon, B. and Newell, P.C. (1991). Accumulation of [³H]-inositol into
- 583 inositol polyphosphates during development of *Dictyostelium*. *Biochem Biophys Res Commun*
- **181:** 191-196.
- 585 Ghosh, S., Shukla, D., Suman, K., Lakshmi, B.J., Manorama, R., Kumar, S. and Bhandari, R. (2013).
- Inositol hexakisphosphate kinase 1 maintains hemostasis in mice by regulating platelet
- polyphosphate levels. *Blood* **122:** 1478-1486.
- 588 Glennon, M.C. and Shears, S.B. (1993). Turnover of inositol pentakisphosphates, inositol
- hexakisphosphate and diphosphoinositol polyphosphates in primary cultured hepatocytes.
- 590 *Biochem J* **293:** 583-590.
- 591 Gokhale, N.A., Zaremba, A., Janoshazi, A.K., Weaver, J.D. and Shears, S.B. (2013). PPIP5K1
- modulates ligand competition between diphosphoinositol polyphosphates and PtdIns(3,4,5)P₃
- for polyphosphoinositide-binding domains. *Biochem J* **453:** 413-426.

- Gueldener, U., Heinisch, J., Koehler, G.J., Voss, D. and Hegemann, J.H. (2002). A second set of loxP
- marker cassettes for Cre-mediated multiple gene knockouts in budding yeast. *Nucleic Acids*
- 596 *Res* **30:** e23.
- 597 Guse, A.H., Greiner, E., Emmrich, F. and Brand, K. (1993). Mass changes of inositol 1,3,4,5,6-
- 598 pentakisphosphate and inositol hexakisphosphate during cell cycle progression in rat
- thymocytes. *J Biol Chem* **268:** 7129-7133.
- Hirumi, H. and Hirumi, K. (1989). Continuous cultivation of *Trypanosoma brucei* blood stream forms
- in a medium containing a low concentration of serum protein without feeder cell layers. J
- 602 *Parasitol* **75:** 985-989.
- Huang, G., Bartlett, P.J., Thomas, A.P., Moreno, S.N. and Docampo, R. (2013). Acidocalcisomes of
- Trypanosoma brucei have an inositol 1,4,5-trisphosphate receptor that is required for growth
- and infectivity. *Proc Nat Acad Sci USA* **110:** 1887-1892.
- Huang, G., Ulrich, P.N., Storey, M., Johnson, D., Tischer, J., Tovar, J.A., et al. (2014). Proteomic
- analysis of the acidocalcisome, an organelle conserved from bacteria to human cells. *PLoS*
- 608 *Pathog* **10:** e1004555.
- 609 Illies, C., Gromada, J., Fiume, R., Leibiger, B., Yu, J., Juhl, K., et al. (2007). Requirement of inositol
- pyrophosphates for full exocytotic capacity in pancreatic beta cells. *Science* **318,** 1299-1302.
- Irvine, R.F. and Schell, M.J. (2001). Back in the water: the return of the inositol phosphates. *Nature*
- 612 *reviews. Mol Cell Biol* **2:** 327-338.
- Jadav, R.S., Chanduri, M.V., Sengupta, S. and Bhandari, R. (2013). Inositol pyrophosphate synthesis
- by inositol hexakisphosphate kinase 1 is required for homologous recombination repair. J Biol
- 615 *Chem* **288:** 3312-3321.
- 616 King-Keller, S., Moore, C.A., Docampo, R. and Moreno, S.N. (2015). Ca²⁺ regulation of
- 617 *Trypanosoma brucei* phosphoinositide phospholipase C. *Eukaryot Cell* **14:**, 486-494.

- Laha, D., Johnen, P., Azevedo, C., Dynowski, M., Weiss, M., Capolicchio, S., et al. (2015). VIH2
- regulates the synthesis of inositol pyrophosphate InsP₈ and jasmonate-dependent defenses in
- 620 *Arabidopsis. Plant Cell* **27:** 1082-1097.
- Lander, N., Cordeiro, C., Huang, G. and Docampo, R. (2016). Polyphosphate and acidocalcisomes.
- 622 *Biochem Soc Trans* **44:** 1-6.
- Lander, N., Ulrich, P.N. and Docampo, R. (2013). Trypanosoma brucei vacuolar transporter chaperone
- 4 (TbVtc4) is an acidocalcisome polyphosphate kinase required for in vivo infection. J Biol
- 625 *Chem* **288**: 34205-34216.
- 626 Li, C., Lev, S., Saiardi, A., Desmarini, D., Sorrell, T.C. and Djordjevic, J.T. (2016). Identification of a
- major IP₅ kinase in *Cryptococcus neoformans* confirms that PP-IP₅/IP₇, not IP₆, is essential for
- 628 virulence. *Sci Rep* **6,** 23927.
- 629 Lonetti, A., Szijgyarto, Z., Bosch, D., Loss, O., Azevedo, C. and Saiardi, A. (2011). Identification of
- an evolutionarily conserved family of inorganic polyphosphate endopolyphosphatases. *J Biol*
- 631 *Chem* **286:** 31966-31974.
- 632 Losito, O., Szijgyarto, Z., Resnick, A.C. and Saiardi, A. (2009). Inositol pyrophosphates and their
- unique metabolic complexity: analysis by gel electrophoresis. *PLoS One* **4:** e5580.
- 634 Luo, H.R., Huang, Y.E., Chen, J.C., Saiardi, A., Iijima, M., Ye, K., et al. (2003). Inositol
- pyrophosphates mediate chemotaxis in *Dictyostelium* via pleckstrin homology domain-
- 636 PtdIns(3,4,5)P₃ interactions. *Cell* **114:** 559-572.
- 637 Luo, H.R., Saiardi, A., Yu, H., Nagata, E., Ye, K. and Snyder, S.H. (2002). Inositol pyrophosphates
- are required for DNA hyperrecombination in protein kinase c1 mutant yeast. *Biochemistry* 41:
- 639 2509-2515.
- Martin, J.B., Bakker-Grunwald, T. and Klein, G. (1993). ³¹P-NMR analysis of *Entamoeba histolytica*.
- Occurrence of high amounts of two inositol phosphates. *Eur J Biochem* **214:** 711-718.

- Mayr GW, R.T., THiel U, Vogel G., Stephens LR (1992). Phosphoinositol diphosphates: non-enzymic
- formation in vitro and occurrence in vivo in the cellular slime mold *Dictysotelium*. *Carbohyd*
- 644 Res 234: 247-262.
- Menniti, F.S., Miller, R.N., Putney, J.W., Jr. and Shears, S.B. (1993). Turnover of inositol
- polyphosphate pyrophosphates in pancreatoma cells. *J Biol Chem* **268**: 3850-3856.
- 647 Moreno, S.N., Docampo, R. and Vercesi, A.E. (1992). Calcium homeostasis in procyclic and
- bloodstream forms of *Trypanosoma brucei*. Lack of inositol 1,4,5-trisphosphate-sensitive Ca²⁺
- release. *J Biol Chem* **267:** 6020-6026.
- Morrison, B.H., Bauer, J.A., Kalvakolanu, D.V. and Lindner, D.J. (2001). Inositol hexakisphosphate
- kinase 2 mediates growth suppressive and apoptotic effects of interferon-beta in ovarian
- 652 carcinoma cells. *J Biol Chem* **276**: 24965-24970.
- Nagata, E., Luo, H.R., Saiardi, A., Bae, B.I., Suzuki, N. and Snyder, S.H. (2005). Inositol
- hexakisphosphate kinase-2, a physiologic mediator of cell death. *J Biol Chem* **280**: 1634-1640.
- Nagata, E., Saiardi, A., Tsukamoto, H., Satoh, T., Itoh, Y., Itoh, J., et al. (2010). Inositol
- hexakisphosphate kinases promote autophagy. *Int J Biochem & Cell Biol* **42:** 2065-2071.
- Nalaskowski, M.M., Deschermeier, C., Fanick, W. and Mayr, G.W. (2002). The human homologue of
- veast ArgRIII protein is an inositol phosphate multikinase with predominantly nuclear
- 659 localization. *Biochem J* **366:** 549-556.
- Nishizuka, Y. (1986). Studies and perspectives of protein kinase C. Science 233: 305-312.
- Oberholzer, M., Morand, S., Kunz, S. and Seebeck, T. (2006). A vector series for rapid PCR-mediated
- 662 C-terminal in situ tagging of *Trypanosoma brucei* genes. *Mol biochem Parasitol* **145:** 117-120.
- Onnebo, S.M. and Saiardi, A. (2009). Inositol pyrophosphates modulate hydrogen peroxide signalling.
- 664 Biochem J **423**: 109-118.

- Pesesse, X., Choi, K., Zhang, T. and Shears, S.B. (2004). Signaling by higher inositol polyphosphates.
- Synthesis of bisdiphosphoinositol tetrakisphosphate ("InsP₈") is selectively activated by
- hyperosmotic stress. *J Biol Chem* **279**: 43378-43381.
- Phillippy, B.Q., Perera, I.Y., Donahue, J.L. and Gillaspy, G.E. (2015). Certain malvaceae plants have a
- unique accumulation of myo-Inositol 1,2,4,5,6-pentakisphosphate. *Plants (Basel)* **4:** 267-283.
- 670 Pisani, F., Livermore, T., Rose, G., Chubb, J.R., Gaspari, M. and Saiardi, A. (2014). Analysis of
- 671 Dictyostelium discoideum inositol pyrophosphate metabolism by gel electrophoresis. PLoS
- *One* **9:** e85533.
- 673 Prasad, A., Jia, Y., Chakraborty, A., Li, Y., Jain, S.K., Zhong, J., et al. (2011). Inositol
- hexakisphosphate kinase 1 regulates neutrophil function in innate immunity by inhibiting
- phosphatidylinositol-(3,4,5)-trisphosphate signaling. *Nat Immunol* **12:** 752-760.
- Resnick, A.C., Snowman, A.M., Kang, B.N., Hurt, K.J., Snyder, S.H. and Saiardi, A. (2005). Inositol
- polyphosphate multikinase is a nuclear PI₃-kinase with transcriptional regulatory activity. *Proc*
- 678 *Nat Acad Sci USA* **102:** 12783-12788.
- Saiardi, A. (2012). Cell signalling by inositol pyrophosphates. *Subcell Biochem* **59:** 413-443.
- Saiardi, A., Caffrey, J.J., Snyder, S.H. and Shears, S.B. (2000). The inositol hexakisphosphate kinase
- family. Catalytic flexibility and function in yeast vacuole biogenesis. *J Biol Chem* **275**: 24686-
- 682 24692.
- Saiardi, A., Nagata, E., Luo, H.R., Sawa, A., Luo, X., Snowman, A.M. and Snyder, S.H. (2001a).
- Mammalian inositol polyphosphate multikinase synthesizes inositol 1,4,5-trisphosphate and an
- inositol pyrophosphate. *Proc Nat Acad Sci USA* **98:** 2306-2311.
- 686 Saiardi, A., Resnick, A.C., Snowman, A.M., Wendland, B. and Snyder, S.H. (2005). Inositol
- pyrophosphates regulate cell death and telomere length through phosphoinositide 3-kinase-
- related protein kinases. *Proc Nat Acad Sci USA* **102:** 1911-1914.

- 689 Saiardi, A., Sciambi, C., McCaffery, J.M., Wendland, B. and Snyder, S.H. (2002). Inositol
- 690 pyrophosphates regulate endocytic trafficking. *Proc Nat Acad Sci USA* **99:** 14206-14211.
- Shears, S.B. (2015). Inositol pyrophosphates: why so many phosphates? *Adv Biol Reg* **57:** 203-216.
- 692 Stephens, L., Radenberg, T., Thiel, U., Vogel, G., Khoo, K.H., Dell, A., et al. (1993). The detection,
- 693 purification, structural characterization, and metabolism of diphosphoinositol
- pentakisphosphate(s) and bisdiphosphoinositol tetrakisphosphate(s). J Biol Chem 268: 4009-
- 695 4015.
- 696 Stritzke, C., Nalaskowski, M.M., Fanick, W., Lin, H. and Mayr, G.W. (2012). A Plasmodium multi-
- domain protein possesses multiple inositol phosphate kinase activities. *Mol Biochem Parasitol*
- **186:** 134-138.
- 699 Szijgyarto, Z., Garedew, A., Azevedo, C. and Saiardi, A. (2011). Influence of inositol pyrophosphates
- on cellular energy dynamics. *Science* **334**: 802-805.
- 701 Ulrich, P.N., Lander, N., Kurup, S.P., Reiss, L., Brewer, J., Soares Medeiros, L.C., et al. (2014). The
- acidocalcisome vacuolar transporter chaperone 4 catalyzes the synthesis of polyphosphate in
- insect-stages of *Trypanosoma brucei* and *T. cruzi. J Eukaryot Microbiol* **61:** 155-165.
- 704 Urbaniak, M.D., Martin, D.M. and Ferguson, M.A. (2013). Global quantitative SILAC
- phosphoproteomics reveals differential phosphorylation is widespread between the procyclic
- and bloodstream form lifecycle stages of *Trypanosoma brucei*. *J Proteome Res* **12:** 2233-2244.
- Verbsky, J.W., Wilson, M.P., Kisseleva, M.V., Majerus, P.W. and Wente, S.R. (2002). The synthesis
- of inositol hexakisphosphate. Characterization of human inositol 1,3,4,5,6-pentakisphosphate
- 709 2-kinase. *J Biol Chem* **277**: 31857-31862.
- Wild, R., Gerasimaite, R., Jung, J.Y., Truffault, V., Pavlovic, I., Schmidt, A., et al. (2016). Control of
- eukaryotic phosphate homeostasis by inositol polyphosphate sensor domains. *Science* **352**:
- 712 986-990.

- Wilson, M.S., Bulley, S.J., Pisani, F., Irvine, R.F. and Saiardi, A. (2015). A novel method for the
- purification of inositol phosphates from biological samples reveals that no phytate is present in
- 715 human plasma or urine. *Open Biol* **5:** 150014.
- 716 York, J.D., Odom, A.R., Murphy, R., Ives, E.B. and Wente, S.R. (1999). A phospholipase C-
- dependent inositol polyphosphate kinase pathway required for efficient messenger RNA export.
- 718 *Science* **285**: 96-100.
- York, S.J., Armbruster, B.N., Greenwell, P., Petes, T.D. and York, J.D. (2005). Inositol diphosphate
- signaling regulates telomere length. *J Biol Chem* **280**: 4264-4269.
- 721 Zhang, T., Caffrey, J.J. and Shears, S.B. (2001). The transcriptional regulator, Arg82, is a hybrid
- kinase with both monophosphoinositol and diphosphoinositol polyphosphate synthase activity.
- 723 FEBS Lett **494**: 208-212.

725 FIGURE LEGENDS

724

726

- 727 Fig. 1. Inositol phosphate pathway in *Trypanosoma brucei*. The soluble IP pathway starts with
- hydrolysis of PIP₂ by TbPI-PLC1, releasing IP₃ that is phosphorylated by TbIPMK to generate IP₄ and
- 729 IP₅. IP₅ is phosphorylated by TbIP5K to generate IP₆. IP₅ and IP₆ can be further phosphorylated by
- 730 TbIPMK or TbIP6K to generate inositol pyrophosphates PP-IP₄ and IP₇. Names of the equivalent yeast
- enzymes are in green.
- Fig. 2. Western blot analyses and enzymatic activity of TbIPMK.
- A. Western blot analyses of *T. brucei* PCF expressing epitope-tagged TbIPMK, TbIP5K and TbIP6K.
- 735 Left panel are HA tagged cell lines: 1, wild-type; 2, TbIPMK-HA; 3, wild-type; 4, TbIP6K-HA. Right
- panel is a c-Myc tagged line: 5, wild-type; 6, TbIP5K-cMyc.

- 737 B. Kinase reactions performed with recombinant TbIPMK (2 μg) using the indicated substrates at 250
- 738 μM for 1 hour at 37°C. TbIPMK can phosphorylate I(1,4,5)P₃ but not I(1,3,4)P₃ to produce I(1,3,4)P₅
- and PP-IP₄, and can phosphorylate I(1,3,4,5)P₄, and I(1,4,5,6)P₄ to produce IP₅ and PP-IP₄. It can also
- phosphorylate I(1,3,4,5,6)P₅ to PP-IP₄. Other *arrows* show bands corresponding to ATP, IP₄, and IP₃.
- TbIPMK can phosphorylate I(1,4)P₂ to produce IP₄, and I(1,4,5)P₃ to produce IP₅ and PP-IP₄.
- 742 C. Treatment of the sample with perchloric acid (PA) eliminates the band corresponding to PP-IP₄ but
- has no effect on IP₆. Other *arrows* indicate bands corresponding to ATP and IP₃.
- 744 D. Optimum pH for TbIPMK activity is within the physiological range.
- E. TbIPMK can only phosphorylate positions 3 and 6 of different IP₅ derivatives to generate IP₆. Note
- the lower synthesis of PP-IP₄ using I(1,3,4,5,6)P₅ as substrate compared to results obtained in (B) and
- 747 (C). We observed that shorter enzymatic reaction time resulted in less PP-IP₄ synthesis.
- All results are representative of three or more independent experiments.
- 750 Fig. 3. *TbIPMK*, and *TbIP5K* complementation of yeast mutants.
- 751 A. HPLC analysis of soluble inositol phosphates of S. cerevisiae arg82∆ mutants transformed with an
- empty vector (red) or a vector containing the entire open reading frame of TbIPMK (blue), and
- compared to those of wild-type (WT) yeast transformed with empty vector (*black*).
- 754 B. Growth of the same cells in liquid medium as estimated by measuring optical density at 660 nm.
- 755 $arg82\Delta$ mutants had reduced growth, which was restored by expression of *TbIPMK*. Mean \pm s.d. for
- three independent experiments, each one with 6 duplicates.
- 757 C. WT, and $arg82\Delta$ transformed with empty vector or $arg82\Delta$ transformed with TbIPMK (serially
- diluted 10-fold, 10⁶-10 cells/spot from left to right) were spotted on YPD plates and incubated at 30°C
- 759 for 2 days.

- 760 D. HPLC analysis of soluble inositol phosphates of $Scipk1\Delta$ mutants transformed with an empty vector
- 761 (red) or a vector containing the entire open reading frame of TbIPMK (blue) and compared with wild
- 762 type transformed with an empty vector (*black*).
- 763 E. HPLC analysis of $Scipk1\Delta Kcs1\Delta$ complemented with empty vector (red) or TbIP5K (green) shows
- reconstitution of IP₆ synthesis. In *black*, wild type transformed with empty vector.
- All results are representative of three or more independent experiments.

- 767 Fig. 4. TbIP6K activity and complementation of yeast mutants.
- A. Kinase reactions performed with recombinant TbIP6K (2 µg) using the indicated substrates at 150
- 769 μM for 1 hour at 37°C. TbIP6K can phosphorylate I(1,3,4,5,6)P₅ to PP-IP₄ and IP₆ to produce IP₇
- 770 (5PP-IP₅) but cannot phosphorylate IP₇ to produce IP₈. Other arrows show bands corresponding to
- 771 ATP, and IP₅.
- 772 B. HPLC analysis of soluble inositol phosphates of S. cerevisiae kcs1∆ mutants transformed with an
- empty vector (red) or a vector containing the entire open reading frame of TbIP6K (blue).
- 774 C. Growth of the same cells in liquid medium as estimated by measuring optical density at 660 nm.
- 775 $kcs1\Delta$ mutants had reduced growth, which was restored by expression of TbIP6K. Mean \pm s.d. for
- three independent experiments, each one with 6 duplicates.
- 777 D. WT, and $kcs1\Delta$ transformed with empty vector or $kcs1\Delta$ transformed with TbIP6K (serially diluted
- 778 10-fold, 10⁶-10 cells/spot from left to right) were spotted on YPD plates and incubated at 30°C for 2
- 779 days.
- 780 E. Optimum pH for TbIP6K activity is under acidic conditions. We detected a higher activity at pH 6.0
- 781 and 6.5.
- All results are representative of three or more independent experiments.

- Fig. 5. HPLC and PAGE analyses of soluble inositol phosphates from *T. brucei* PCF and BSF.
- A. PCF showed the presence of IP, IP₂, IP₃ and IP₆.
- 786 B. BSF showed the presence of IP, and IP₂. Cells were labeled with [³H]inositol as described under
- 787 Experimental Procedures.
- 788 C-E. PAGE analyses of extracts from PCF (C) or BSF (D) or standard IP₆ (E). Samples in (C) and (D)
- 789 (5 x 10⁹ cells) were treated with phytase (Phy) (0.1 mg/ml, pH 5.0, at 37°C for 1 hour) to confirm that
- 790 the bands correspond to IP_6 .
- E. Phytase control activity with IP₆ standard.
- All results are representative of three or more independent experiments.
- 793
- Fig. 6. Phenotypic changes of mutant BSF deficient in TbIPMK.
- A. qRT-PCR analysis of gene expression of *TbIPMK* at time 0 and after 1 and 3 days in the absence of
- tetracycline as compared to expression of control actin. Values are means \pm s.e.m., n = 3. P < 0.001 at
- 797 days 1 and 3 without tetracycline. Student's *t* test.
- 798 B. In vitro growth of BSF in the presence (+Tet) or absence (-Tet) of 1 μ M tetracycline. Values are
- means \pm s.e.m., n = 3 (bars are smaller than symbols).
- 800 C. Quantification of short-chain polyphosphate in control (+Tet) and induced (-Tet) TbIPMK
- 801 conditional knockout BSF. Values are means \pm s.e.m, n = 3, *P < 0.05. Student's t test.
- 802 D. Numeric distribution of acidocalcisomes in BSF. Whole unfixed parasites were observed by
- 803 transmission electron microscopy and the number of acidocalcisomes per cell in ~100 cells of control
- 804 (+Tet) and conditional TbIPMK mutants (-Tet) were counted (the results from 3 independent
- 805 experiments were combined).
- 806 E, F. Scanning transmission electron microscopy (STEM) images from control (E) or TbIPMK
- 807 conditional mutant BSF showing acidocalcisomes. Bar = 1 µm. Insets show acidocalcisomes
- highlighted in (E) and (F) at higher magnification. Bars = $0.5 \mu m$.